Stony Brook University

Structure Prediction of Carbon Dioxide Hydrate and Xenon Hydrate

A Thesis Presented

by

Hongfei Xu

to

The Graduate School

in Partial Fulfillment of the

Requirements

for the Degree of

Master of Science

in

Geosciences

Stony Brook University

May 2014

Stony Brook University

The Graduate School

Hongfei Xu

We, the thesis committee for the above candidate for the

Master of Science degree, hereby recommend

acceptance of this thesis.

Artem R. Oganov – Thesis Advisor
Professor, Department of Geosciences

Brian Phillips – Second Reader
Professor and Graduate Program Director, Department of Geosciences

Lars Ehm – Third Reader
Research Associate Professor, Mineral Physics Institute

This thesis is accepted by the Graduate School

Charles Taber
Dean of the Graduate School

Abstract of the Thesis

Structure Prediction of Carbon Dioxide Hydrate and Xenon Hydrate

by

Hongfei Xu

Master of Science

in

Geosciences

Stony Brook University

2014

Gas hydrate technology is one of research focus in recent years, and can be applied to solve problems in energy, environment, and other areas. Previous views had been that most gas hydrates decompose into gas and water (or ice) under 1 GPa or so, thus, research on hydrate structures in past few decades were conducted under low pressure conditions. Recent studies have shown the possibility that new structures of gas hydrate may exist under higher pressure, and this thesis aims to explore the structures of hydrate in carbon dioxide-water system and xenon-water system with the application of high pressure.

The evolutionary algorithm USPEX combined with first-principle calculation is applied in this study. The main research contents include the prediction of gas hydrate structures in certain conditions performed by USPEX codes, and the analysis of their physical properties. In the carbon dioxide-water system, structures are predicted under 5 GPa, by variable composition calculation. The results demonstrate that there's no thermodynamically stable structure of carbon dioxide hydrate under that condition. Properties of some typical structures ($CO_2 \cdot 7H_2O$, $CO_2 \cdot 4H_2O$), which cannot stably exist in this system, are analyzed to explain the

decomposition. In the xenon-water system, variable composition calculation are performed under 10 GPa, 20 GPa and 50 GPa, respectively. The results show the existence of metastable structure of xenon hydrate which can be indexed as $2Xe \cdot 8H_2O$ under 10 GPa. The data also illustrates there's no thermodynamically stable structures under 20 GPa and 50 GPa. To further study the structure of xenon hydrate, fixed composition calculation of $2Xe \cdot 8H_2O$ is conducted under 5 GPa and 10GPa, and the physical properties of that structure are investigated and described in the thesis.

Contents

List of Figures

List of Tables

Chapter 1

Introduction of Gas Hydrate

Environment, energy and life science have become issues to which people pay more and more attention, and gas hydrates demonstrate huge application prospect in these areas. Natural gas hydrate with methane as the main component occurs in the broad continental shelf, which is regarded as a considerable resource to relieve energy crisis; carbon dioxide rapidly increasing in the air could be put into clathrate water molecules and sunk to the bottom of the ocean to lessen greenhouse effects; the formation process of hydrate can be applied to effectively dissociate gas and reduce pollution. It thus appears that gas hydrate shows a promising future in diverse domains.

Although gas hydrate has significant value in engineering application and scientific research, its crystal structure, bonding mechanism, pressure-temperature phase diagram, thermal chemical and mechanical stability, the reaction kinetics of synthesis and decomposition, and others properties still need further research. Currently, scientists have studied and discussed ways to organically combine the prediction in high-pressure or low-temperature environment with laser spectrum, thermal measurement and other technologies, so as to conduct a series of experimental research to solve many basic scientific problems. Methane, carbon dioxide, and some noble gas hydrates in high-pressure environment show huge advantages in research, and great progress has been achieved in confirming the hydrate crystal structure, and the occupancy of gas molecule in hydrate lattice.

1.1 Research development of gas hydrate

Gas hydrate, also named as clathrate hydrate, is a kind of crystalline compounds of non-stoichiometric type formed by water and small gas molecules.[1]

From 1810, when Davy found hydrates for the first time, people have conducted a lot of experiments and theoretical research.[2] In the first 100 years, people's interest in hydrate basically is academic. The main research content is confirming which gas can produce hydrates and the temperature and gas condition for the generation. Since Hammer-Schimidt discovered the reason for the blocking of natural gas processing equipment and pipelines is

the generation of gas hydrates instead of freezing, how to suppress or prevent the formation of gas hydrates has become an urgent problem to be solved in the petroleum gas industry.[3] After the 1960s, research on gas hydrate have expanded to multiple fields: Russian scientists predicted that the natural gas hydrate probably exists on the surface of the bottom of the ocean, and discovered a natural gas hydrate layer in Siberian tundra. As a kind of potential energy source, natural gas hydrate has aroused great interest from each country's government, industry and scientists; some people try to use hydrate to study sea water desalination, dangerous substances storage and environment governance. In June, 1993 and June, 1996, two special international conferences on gas hydrate were separately convened in New York and Toulouse, marking the research on hydrate has entered into a new stage of vigorous development. The conference papers included work on the structure and performance of hydrate, the formation and decomposition dynamics, formation hydrate energy utilization, new materials and many other fields, and explained how extensive research on hydrate is significant for chemical industry, energy industry, environment protection industry, etc.

1.2 The main structure types of gas hydrate

Gas hydrate is a kind of compound in clathrate structure generated by reaction between water and gas molecule under certain temperature, pressure, gas saturability, pH and other conditions. It can be represented by $M \cdot nH_2O$, of which M represents the gas molecule in the hydrate, and n is the number of water molecules.[4] In recent years, it has been found that some clathrate hydrates are made of small molecule gases (such as nitrogen, methane, etc.), while some are made of large molecule (such as THF). However, all these gas hydrates have a common point, gas molecule ('guest') occupies the'host'cage formed by hydrogen bonding between water molecules.

These structures of such hydrates are stable because of : (1) the attraction between water molecules of clathrate hydrate; (2) the repulsion produced by the hydrophobic nature of host and guest materials.[5]

Further research shows that there are mainly four kinds of gas hydrate structure, i.e. CS-I, CS-II, SH and ST. The hydrate in CS-I type is a cubic crystal structure, which only accommodates methane, ethane, N_2, CO_2, H_2S and other non-hydrocarbon molecules, and its

space group is *Pm3n*. CS-I has two kinds of cages (**Fig.1**), and each unit cell contains 2 pentagonal cages and 6 large cages made up of hexagons and pentagons. In addition, the proportion of water and guest of CS-I is 46:8 (or 5.75:1).

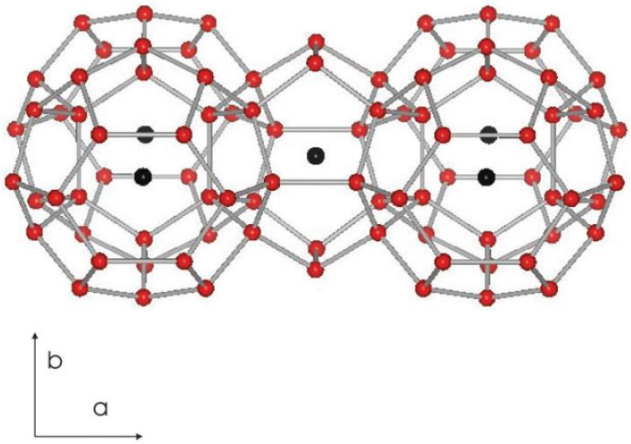

Fig. 1 The structure of cubic structure I (CS-I) clathrate hydrate. The red balls represent the oxygen atoms of the host water molecules and the black balls mark the centers of the guest molecules. [6,7]

The hydrate of CS-II is a tetragonal crystal structure, which can accommodate bigger gas molecules, and its space group is *Fd3m*, and has two kinds of cages (**Fig.2**). In each unit cell, there are 16 pentagonal small cages and 8 big cages made up of pentagons and hexagons.As there are 136 water molecules per unit cell, the proportion of water and guest is 5.66:1.

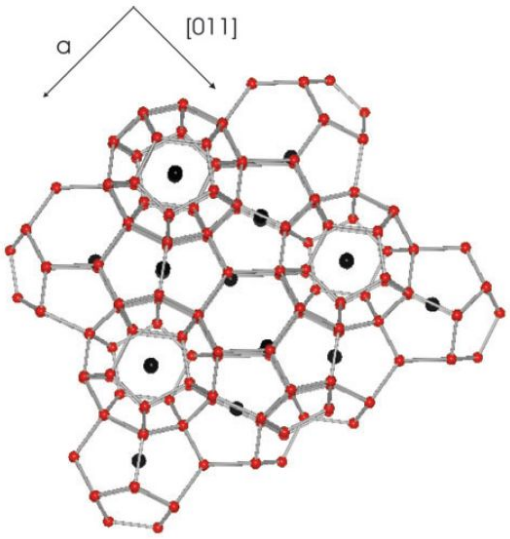

Fig. 2 The structure of CS-II clathrate hydrate. The red balls represent the oxygen atoms of the host water molecules and the black balls are the centers of the guest molecules.[8]

The hydrate of SH type is a hexagonal crystal structure, which was first discovered in the dimethylpentane–Xe–H_2S water system.[9] Except for the aforesaid micromolecule, the structure also can accommodate larger molecules with diameter of 7.5~8.6Å. ST type hydrate was firstly found in pinacol–water system, and it is a tetragonal structure.[10]

According to previous researches, hydrate of CS-I type is the distributed most widely in nature, while CS-II and SH turn out to be more stable. Studies also found that hydrates of CS-I type mostly are biogenic methane hydrates, while CS-II and SH hydrates are pyrolysis products. Under low pressure, CS-I and CS-II are the main structure of gas hydrate, while SH and ST are more likely to occur in high-pressure conditions. Under extremely high pressure, gas hydrate will present hydrogen bonding network structure, which is related to ice *Ih*, so that it is called FIS (filled-ice structure).[11]

1.3 Influence of pressure on gas hydrate

Dissociation behavior is very common in gas hydrates, of which the dissociation curve of methane hydrate is typical.(**Fig.3**)

Take methane hydrate dissociation curve as an example. At 0-0.5 GPa (194K-320K), the dissociation temperature will rapidly arise with the increase of pressure, the reason for which is that the molar volume of clathrate under low pressure is much less than the equivalent volume of ice (or water) and gas.[12] When the pressure increases, the volume difference (that is ΔV) starts to decrease, because gas is more easily compressed than water and clathrate, hence, the slope in the curve declines. Under higher pressure, there is much more dissociated methane-water mixture than clathrate, so ΔV falls to a negative value. The slope of the dissociation curve in the figure can be described by $\mathrm{d}T_d/\mathrm{d}P=\Delta V/\Delta S$, in which T_d represents dissociation temperature. When the dissociation temperature is lower than the melting temperature of ice (1.25 GPa，305 K), ΔS (entropy change) becomes smaller, because in this condition, clathrate is easier to form ice rather than liquid water. Therefore, $\mathrm{d}T_d/\mathrm{d}P$ becomes much larger and the dissociation temperature will rapidly drop to 0 K upon calculation. Although the result is not perfect, this model has described well the formation of clathrate and its stability under low pressure, and it is widely viewed to be applicable for other gas hydrates. Hence, at that time, many research held that pressure of 1 GPa or even higher

pressure would lead all clathrate hydrates to become unstable.[13]

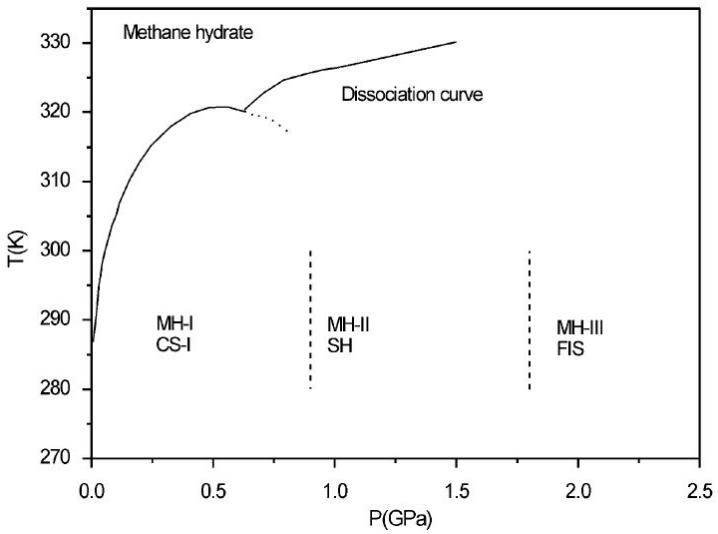

Fig. 3 The phase diagram of methane hydrate. The solid line shows the dissociation curve, while the dotted line shows the phase boundary. This curve was determined by Dyadin *et al*.

Researches on gas hydrate beyond the pressure range of the theory described above started to be studied in recent years. In the late1990s, Dyadin *et al.* conducted a series of studies on the dissociation curve of gas hydrate above 1.5 GPa pressure, of which many researches showed that new structures probably exist under higher pressure.[14-18] Closer microscopic methods revealed that some gas hydrates have stable structures up to 90 GPa or higher pressure.[19] These studies have changed people's understanding of gas hydrate behavior under high temperature, and demonstrated the research prospect of gas hydrate structure under high pressure.

Chapter 2

Methods and Principles

In this thesis, the structure prediction process is conducted by USPEX codes, and analysis of the properties is performed by quantum mechanics programme which is designed on the basis of DFT and First Principles. The characteristics of USPEX and relevant theories will be elaborated in this chapter.

2.1 Introduction of crystal structure prediction

Crystal structure is the most basic property for people to profoundly learn crystalline materials; it plays a particularly important role in revealing the relationship between the material microstructure and intrinsic properties such as elasticity, electrons, phonons, vibration and thermodynamics, etc. Although the microstructures of crystals can be confirmed by such means as X-ray diffraction, etc. in experiments, the microstructures of crystals confirmed by experiments face severe challenges due to restrictions on the experimental measurement such as the purity of the sample, the size of the diffraction signal and insufficient experiment conditions, in particularly under some extreme conditions (such as high pressure). Therefore, predicting the crystal structure under certain conditions through theoretical calculation without relying on any experimental result is of important scientific significance and engineering application value for finding new materials and exploring specific physical properties.

Density Functional Theory (DFT) which is based on First Principles is playing an increasingly important role in crystal structure prediction and property computation for materials. Crystal structure is the basis for carrying out research on the physical properties of materials; therefore, how to correctly and effectively predict crystal structure is the starting point for the problems that we research. Currently, the known prediction methods for crystal structure mainly consist of three kinds: the first kind is random search method. Since anatomic arrangement configuration is almost an astronomical figure, this method has low search efficiency or needs to rely on the experiential knowledge of crystal structure units. The second kind is minima hopping and megadynamics.[20,21] The shortcomings of this method lie in that the finally predicted structure highly relies on the initial structure. The last kind of

method is evolutionary algorithm based on biological heredity. The advantages of this method include fast convergence, high precision, large search range and only needing the chemical constituents without relying on the initial structure.

In 1988, John Maddox, Chief Editor of *Nature,* once published an editorial on *Nature*, stating that one of the most important challenges in Physics is to confirm crystal structure according to chemical constituents. Most researchers still thought that crystal structure is as unpredictable as the earthquake until 1980s~1990s.[22,23] In 1990, French Pannetier *et al.* proposed a method for predicting inorganic compounds by simulated annealing method. In the same year, Catlow *et al.* from University College London proved the feasibility of computer prediction for the crystal structure of materials and provided the basis for the calculation method.[24,25] In 1996, German Schmidt *et al.* predicted the molecular structures of metallo-organic compounds by means of interatomic potentials method.[26] During 2003~2006, revolutionary progress was achieved in the field of crystal structure prediction; and people's knowledge on crystal structure prediction changed to a great extent accordingly. In recent years, a large number of literatures and reports have researched many new materials and properties by different methods for crystal structure prediction, which makes crystal structure prediction comes true. Currently, some foreign research groups are researching the prediction for crystal structure. Jansen and Schön *et al.* from German Max Planck Institute put forward the concept of energy landscape in chemical system and programed G42, a program for structure prediction.[27-30] They searched the phase structure which may exist in material system by means of global optimization algorithm for energy by combining empirical potential and simulated annealing algorithm; then they further optimized the position with locally minimum on the potential energy surface, thus searching the phase structure existing in such material system. This provides a feasible method for predicting the phase structure of new materials, and provides theoretical guidance for synthesis process route for these compounds in future. Lufaso and Woodward *et al.* from University of North Florida programmed SPuDS, a software package specialized in predicting perovskite structure.[31] Bail from Universite Du Maine developed GRINSP (geometrically restrained inorganic structure prediction), a program for predicting inorganic crystal structure.[32] This software can search the arrangement structure of binary or ternary inorganic compounds in

three-dimensional space by means of Monte Carlo method. Mellot–Draznieks *et al.* developed AASBU (automated assembly of secondary building units) software package for structure prediction by alternate using simulated annealing and energy minimization via Cerius2 and GULP software.[33,34] Oganov *et al.* from our group developed USPEX (Universal Structure Predictor: Evolutionary Xtallography), a software for crystal structure prediction. This software can predict the structures of crystals only with the chemical constituents of the material under any pressure condition. In addition, USPEX also has many other characteristics: it can predict the stable and metastable phase structures of the materials; it can predict the structure and surface reconstruction of nano-particles; it provides interfaces with software such as VASP, GULP, DMACRYS, CP2k, QuantumEspresso and CASTEP, etc.; it displays the computation results in a graphical manner via powerful visualized analysis software STM4; it provides many algorithms for structure search, such as USPEX algorithm, random sampling method, metadynamics algorithm, minima hopping algorithm. Apart from energy optimization, it can also compute other physical properties of the materials, such as hardness, density and various electronic properties. Currently, there are over 1200 researchers using USPEX software to carry out scientific researches all over the world, and they have successfully predicted many new structures and new properties. For instance, Zhu *et al.* have predicted several allotropes of carbon by this method, they are denser than diamond;[35] Wen *et al.* have managed to predict the structure of graphane, a two-dimensional hydrocarbon;[36] Oganov, *et al.* have predicted and synthesized a superhard high-pressure phase ion material γ–B28 through theories and tests;[37,38] the results of an unprejudiced test for crystal structure prediction indicate that USPEX is superior to other methods in terms of computing efficiency and reliability.[39]

2.2 Method description: evolutionary algorithm USPEX

2.2.1 Basic terms

Population: a series of points in the search domain, i.e., crystal structure which may exist in optimization procedure.

Parent generation: individuals with good fitness value in the population which are selected to generate the next generation of the population.

Off-springs: solutions obtained by genetic manipulation of the parent generation in the population.

Selection: determining whether to “survive” or “weed out” different structures.

Heredity: the two individuals selected in the parent generation each contributes a piece of section to recombine and generate the alternative structure of the next generation, while the lattice parameters of the new structure of the filial generation is obtained by adding the cell parameters and random weight of the two parents structures.

Mutation: artificially change the lattice parameters or atom sites of the parent generation structure to generate new structure for the next generation.

Permutation: when there is more than one atom type in the parent generation, the optimum atomic arrangement method can be obtained by randomly permuting the positions of different types of atoms.

2.2.2 Basic flow of evolutionary algorithm

Fig.4 has shown the basic flow of evolutionary algorithm. In this part, the operation and important parameters of USPEX will be described.

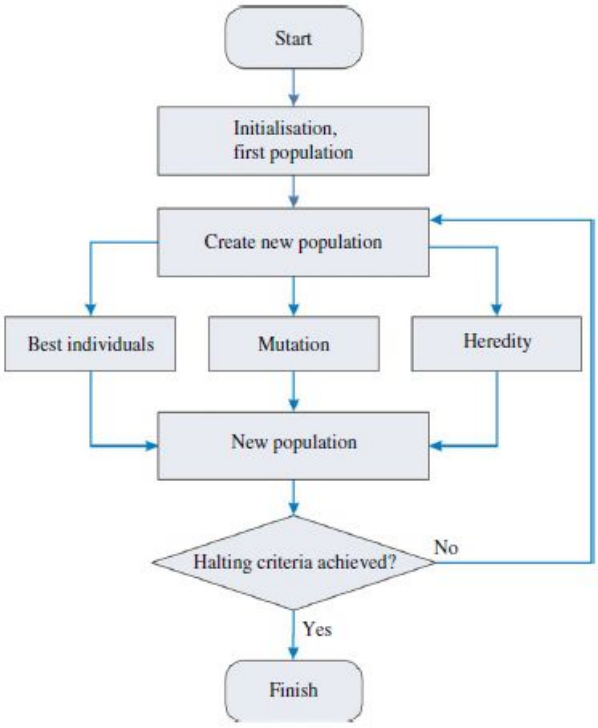

Fig. 4 flow of evolutionary algorithm [40]

Local optimization and restriction

Crystal structure is defined by two kinds of floating-point number parameters of lattice parameters and atomic coordinates; it includes 6 lattice parameters, 3 lattice vectors and 3 included angles (α, β, γ) whose value ranges are within [0, π]. There are three fractional coordinates corresponding to the exact lattice basis vector for each atom. Therefore, a group of values are defined as a structure, a locally optimized structure is individuals, and a group of individuals constitute a population or a generation. The work flow for this method is as follow: using the parent generation structures selected from all the structures in any generation to generate a new candidate structure for the next generation by means of one or several operations of the following three permutations, i.e. heredity, mutation and permutation. Any candidate structure generated during the aforesaid prediction process must meet the following three conditions: (1) the distance between two atoms shall be larger than the preset value; (2) the included angles between lattice basis vectors shall be between 60° and 120°; (3) the length of unit cell shall be larger than the given value. Meeting the aforesaid three constraint conditions can ensure the stability of total energy calculation and local optimization and remove the redundant nonphysical structures, so as to guarantee the excellence and reasonability of the next generation structure.

Initial population

USPEX generates the initial population by random sampling method. Under the condition of lacking of understanding of optimized structure, random sampling method can objectively search the crystal structure in the entire solution space; meanwhile, random sampling can ensure the diversity of the population, while the high diversity of initial population is the key to the success of evolutionary algorithm. However, under some circumstances, unit cell information such as lattice parameters or unit cell volume is known, therefore, they can be set as constraints. For instance, if lattice parameters are known, then the lattice parameters can be fixed and only the positions of the atoms in the unit cells are changed. Reasonable structure can also be put in the first generation by “seed technique”, with the remained part filled by random structures.

The diversity of initial population is the key to the success of evolutionary algorithm. However, simple random sampling cannot ensure the high efficiency of crystal structure

prediction. USPEX ensures the diversity and randomness of the population by means of unit cell division. Unit cell division refers to subcells divided from a large unit cell; then they will constitute an entire unit cell through duplication, its high translation symmetry and order can ensure the diversity of the population. For the structures which are not suitable for dividing into subcells, USPEX algorithm will generate random vacancies in the unit cells, so as to ensure the correct atom numbers in the unit cells. This method will not introduce extra symmetry. When processing large system, this method can effectively increase the diversity.

Operators

USPEX evolutionary algorithm uses three operators: heredity, lattice mutation and permutation. Heredity: the two individuals selected in the parent generation each contributes a piece of section to recombine and generate the off-spring generation, while the lattice parameters of the new structure of the filial generation is obtained by adding the cell parameters and random weight of the two parents structures (**Fig. 5a**). Lattice mutation: artificially change the lattice parameters of the parent structure to generate new structure for the next generation (**Fig. 5b**). Permutation: when there is more than one atom type in the parent generation, the optimum atomic arrangement method can be obtained by randomly permuting the positions of different types of atoms (**Fig.5c**).

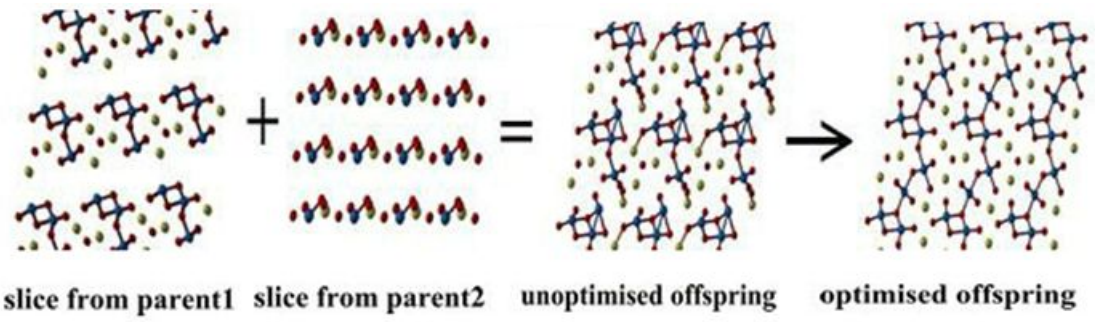

(a)

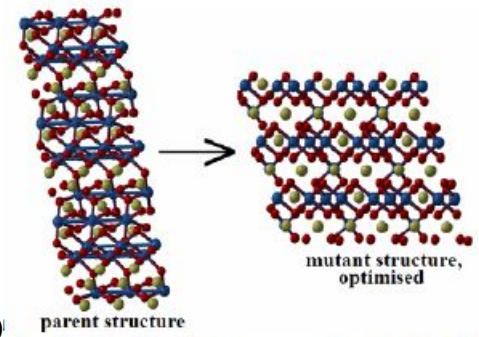

(b)

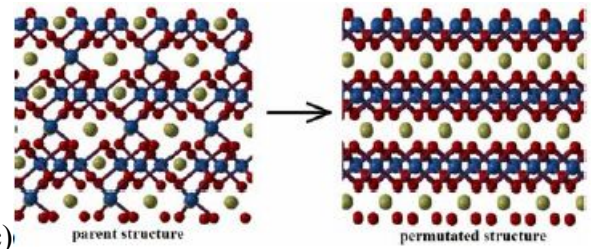

(c)

Fig. 5 (a) Heredity; (b)lattice mutation ; (c)permutation. [41]

The aforesaid three operators carry out combinatorial optimization for different structures in the search space, so as to preserve and extract its dominant spatial features through genetic evolution of each generation, and finally obtain the optimum crystal structure.

Survival of the fittest

USPEX evolutionary algorithm determines how many individuals in the next generation will "survive" by setting probability value. After applying operators, USPEX evolutionary algorithm will firstly compute the target values (energy, hardness and density, etc.) in different individuals by mean of target value function, then rank the sizes of these individual target values. By setting probability value, if the worst 40% is weeded out, then the best 60% will be selected as the parent generation to keep to the next generation. Fitness function determines the "survival" probability of different individuals; high fitness generally means the high possibility of being selected as parent generation, therefore, its probability of being inherited to the next generation will be larger. Apart from selection by means of fitness function, USPEX evolutionary algorithm also adopts random selection to some extent since random selection can maintain the diversity of the population, which is conducive to avoiding the algorithm from falling into local minimum.

Termination rule

After generating the new generation, firstly, the evolutionary algorithm will optimize the structure; after the optimization, it shall create the next generation by selection and mutation operation, this process shall be repeated until it meets the termination standard. Under general conditions, free energy shall be selected as the target value function. Therefore, the individuals with low energy (chemical thermodynamics enthalpy) will be selected as the next generation structure, then this process shall be repeated until the free energy cannot mutate anymore or reaches the set genetic algebra. Obviously, termination rule shall undergo a certain amount of genetic algebras. When the population is fully filled with optimum structure or reaches the set target value or meets the preset genetic algebra; these standards can be the standards for terminating the evolutionary algorithm, which shall be determined by the specific structures to be solved. All in all, the termination rule for USPEX is to search the

optimum structure to meet the users' demand.

Fingerprint function

One of the largest defects of the evolutionary algorithm is early convergence, i.e., evolutionary algorithm is prone to falling into some local minimum instead of global minimum during implementation process. The reason for this lies in that the optimum structure is prone to generating offspring near it; this mechanism will reduce the diversity of the population by means of duplicating its own structure and filling its neighborhood structures. In particularly when there are many excellent local minimums in energy landscape, early convergence will be very common. Therefore, fingerprint function is used for maintaining the diversity of the population, so as to avoid early convergence.

Firstly, a method is needed to distinguish and measure the similarities of different structures. Directly comparing the coordinates of the atoms or comparing the differences between free energies can neither effectively distinguish them; the coordinates of the atoms are represented by lattice vectors which rely on the unit cells selected, while the selection methods for unit cells are various. Free energies in the search space are chaotic instead of monotonous; therefore, it cannot measure the similarities of different structures. An ideal way is to distinguish the differences at the same position due to atom permutation or small numerical value difference. USPEX describes the crystal structure by fingerprint function technique which is a function similar to radial distribution function (RDF) and diffraction spectrum. It is defined as:

$$f(R) = \sum_i \sum_{j \neq i} \frac{Z_i Z_j}{4\pi R_{ij}^2} \frac{V}{N} \delta(R - R_{ij}) \qquad (1)$$

Z_i is the quantity of atom i, R_{ij} is the distance between atom i and j, V represents the volume of unit cell, N is the total atomicity of a unit cell. Attention: R is a variable instead of a parameter. To eliminate the dependence of the fingerprint on the truncation distance, the fingerprint function is normalized to be:

$$f_n(R) = \frac{f(R)}{\sum_{i,j} Z_i Z_j N_i N_j} - 1 \qquad (2)$$

Describing crystal structure by fingerprint function is featured by all the expected properties

as mentioned above. Firstly, fingerprint function doesn't rely on the coordinates of the atoms and only relies on the interatomic distance; therefore, selection of unit cells won't affect fingerprint function f（R）. Small disturbance at the atom sites has a small influence on the fingerprint function; meanwhile, atomicity shall be used as the weighting coefficient to consider the arrangement of the atoms. Similarly, the similarities of the two structures can be measured by calculating the distance of fingerprint function; cosine distance is used in USPEX, and Cartesian distance or Minkowski norm can also be used. To simplify and accelerate the computing, USPEX discretizes fingerprint function f（R） and represents it as vector FP and refers to it as fingerprint.

$$FP_i(R) = \frac{1}{D} \int_{iD}^{(i+1)D} f_n(R) dR \tag{3}$$

The cosine distance between the two fingerprint functions of structure i and j is defined as:

$$d_{ij} = 0.5\left(1 - \frac{FP_i FP_j}{\| FP_i \| \| FP_j \|}\right) \tag{4}$$

The similarities of different structures can be judged by the distance defined in fingerprint function space.

2.3 First Principles and Density Functional Theory

2.3.1 First Principles calculation method

The interaction among atoms in solids directly determines the basic property of the material. Currently, the methods for researching materials in micro field mainly include Monte Carlo method, Molecular Dynamics method and First Principles calculation method, where Monte Carlo method and Molecular Dynamics method are mainly based on classical theory, while First Principles calculation method is based on electron theory in Quantum Mechanics.

First Principles are established on the basis of Born-Oppenheimer approximation, nonrelativistic approximation and single electron approximation, including Hartree-Fock theory, post Hartree-Fock theory and DFT, etc. Based on Quantum Mechanics principles, it can directly solve Schrodinger equation which describes the movement of microscopic

particles without using any free parameter, so as to obtain property information related to the electronic structures and atomic structures of the materials, thus understanding the physical and chemical phenomenon in the materials from more micro essence. First Principles can accurately predict the properties of materials even before the manufacturing of new materials; therefore, it is an indeed prediction which can guide the innovative design of materials. This method is also referred to as *ab initio* method.

First Principles calculation method starts from the most basic and the simplest physical facts, since its computing results have high precision and reliability, it has become another knowhow for researching material structure and property independent of laboratory. When processing the interaction of multiple electron systems, First Principles calculation often needs to make the approximations to some extent; however, such approximations are all gained by physically assumption and mathematically reasonable simplification. For instance, modern theory "single electron approximation" develops on the basis of Density Functional Theory (DFT); DFT which is based on First Principles method can better process the interactions among electrons including permutation-correlation interactions, and analyzes various physical properties of solids by combining total energy calculation technique. This is a method with strong theoretical property developing from Quantum Mechanics and Theory of Solids; and it can be used for researching crystalline materials with periodicity or solids with abundant atoms. This method has been widely used in material science field so far. The calculation method used in this paper is Density Functional Theory based on First-principles. Hartree–Fock method deems the electrons to be discussed as moving in ion potential field and the mean potential field of other electrons, however, it ignores the permutations and related effects among other electrons, which limits the computing precision to some extent. Density Functional Theory skillfully expresses the permutations among electrons as the functional of electron density, thus enabling Schrodinger equation to be solved by means of self-consistent method after considering the complicated interaction among electrons. When actually solving Kohn–Sham equation, people adopt different technical processing means and develop many different solving methods in line with the different material systems or the different properties of the researched materials. These methods can be classified by considerations of various parts of effective Hamiltonian quantity of Kohn–Sham equation and

wave function constructions. Different approximation schemes are proposed on the basis of permutation-correlation functional, such as Local Density Approximation (LDA) and Generalized Gradient Approximation (GGA).[42] For the different basis sets which can be selected for wave function, there are atomic orbital basis sets (GTO, STO and Dmol, etc.), plane wave basis set (PW), Augmented Plane Wave (APW), etc. For atomic nucleus potential, full-electronic computing, full-electronic Muffin–tin potential and Pseudopotential, etc. can be selected. For kinetic energy items, relativity theory, semi-relativistic theory and non-relativistic theory forms can be taken.[43]

First Principles are mainly used for researching the properties of materials on electron level. The total energy, charge distribution (charge density and state density) and energy band structure of the system can be obtained by directly solving Schrodinger equation of multiparticle system. Based on this, many basic physical properties such as elastic property and phonon property, etc. of the crystalline materials can be calculated through prediction.

2.3.2 Density functional theory

Density functional theory (DFT) is a quantum mechanics method used to study electronic structure of multi-electron system. DFT has been widely applied to physics and chemistry. Especially, it is used to study nature of molecule and condensed state and acts one of the most common methods in the field o condensed matter physics and calculational chemistry. With establishment of quantum theory and development of computer technology, people hope to get numerical solutions to quantum mechanics equations of microcosmic system by virtue of computer. However, solutions to Schrodinger's equation are extremely complicated. One theoretical leap that overcomes this complexity is DFT.

DFT derives from Thomas-Fermi model. However, there was no solid theoretical basis until Hohenberg-Kohn theorem was proposed. Tradtioal quantum theory uses wave function as fundamental physical quantity, while DFT describes physical property of system ground state by particle density. Because electron wave function has $3N$ variables (N is the number of electrons and each electron contains three spatial variables) but electron density is just a function of three variables, its processing is more convenient in both concept and practice. Besides, DFT is a theory that is completely based on *ab initio* of quantum mechanics. In

order to distinguish it from other *ab initio* methods of quantum chemistry, people usually call the calculation based on DFT First-principles calculation.[44,45]

The most common application of DFT is realized by Kohn-Sham method. In the framework of Kohn-Sham DFT, complicated many-body problems (caused by mutual effect of electrons staying in one external electrostatic potential) are simplified as a problem about movement of electrons without mutual effect in an effective potential field. The effective potential field includes impacts of external potential fields and Coulomb interaction among electrons, such as exchange and correlation.[46,47] Processing exchange and correlation is a difficult point of K-S DFT. Up to now, there have been no ways to solve exchange-correlation energy accurately.

In common calculation about electronic structure of many-body problems, nucleus can be considered to stationary (Born - Oppenheimer approximation). In doing so, it can be seen that electrons move in the electrostatic potential V generated in nucleus. Stationary state of electrons can be described by $\psi(\vec{r_1},\cdots,\vec{r_N})$ the wave function that satisfies multi-body Schrodinger's equation:

$$H\psi = [T+V+U]\psi = [\sum_{i}^{N} -\frac{h^2}{2m}\nabla_i^2 + \sum_{i}^{N} V(\vec{r_i}) + \sum_{i<j} U(\vec{r_i},\vec{r_j})]\psi = E\psi \tag{5}$$

Where N is the number of electrons and U is interaction potential among electrons. The operators T and U are called pervasive ones and the same in all systems, while the operator V depends on system and is called non-pervasive operator. It can be found that the difference between single-particle problems and complicated multi-particle problems lies in the exchange interaction item U. Up to now, there have been many mature methods used to solve multi-body Schrodinger's equation. DFT converts multi-body problems containing U into one-body problems that do not contain U, so it becomes an effective way to solve this kind of problems. In DFT, the most critical variable is particle density $n_0(\vec{r})$ which is given by the following formula:

$$n(\vec{r}) = N\int \mathrm{d}^3 r_2 \int \mathrm{d}^3 r_3 \cdots \int \mathrm{d}^3 r_N \Psi^*(\vec{r},\vec{r}_2,\ldots,\vec{r}_N)\Psi(\vec{r},\vec{r}_2,\ldots,\vec{r}_N) \tag{6}$$

Conversely, $\psi(\vec{r_1},\cdots,\vec{r_N})$ the corresponding ground-state wave function can be calculated in

principle given ground-state electron density $n_0(\vec{r})$. In another word, ψ_0 is the only functional, i.e.,

$$\Psi_0 = \Psi_0[n_0] \tag{7}$$

Accordingly, O observable quantity of all other ground states is functional of n_0.

$$\langle O \rangle [n_0] = \langle \Psi_0[n_0] | O | \Psi_0[n_0] \rangle \tag{8}$$

Then, we can obtain that ground-state energy is functional of n_0 as well.

$$E_0 = E[n_0] = \langle \Psi_0[n_0] | T + V + U | \Psi_0[n_0] \rangle \tag{9}$$

In detail, $\langle \Psi_0[n_0] | V | \Psi_0[n_0] \rangle$ contribution of external potential fields can be expressed as follows by using density.

$$V[n] = \int V(\vec{r}) n(\vec{r}) \mathrm{d}^3 r \tag{10}$$

T[n] and T[n] are called pervasive functional, while it is obvious that V[n] is not pervasive, which depends on the considered system. For the confirmed system, i.e., V is known, it is necessary to solve minimal value of $n(\vec{r})$ for the functional.

$$E[n] = T[n] + U[n] + \int V(\vec{r}) n(\vec{r}) \mathrm{d}^3 r \tag{11}$$

Here, it is assumed that expression of T[n] and U[n] can be obtained. By solving extreme value for energy functional, we may obtain the ground-state energy n_0 and then solve observable quantity of all ground states.

When variational extreme value of the energy functional E[n] is solved, we may use Lagrange method of indefinite operators, which was finished by Kohn and Sham in 1965. Here, we use the following conclusion: the functional in the foregoing equation can be expressed as an energy functional without interaction system.

$$E_s[n] = \langle \Psi_s[n] | T_s + V_s | \Psi_s[n] \rangle \tag{12}$$

Where T_s is the kinetic energy without interaction, and V_s is external potential fields that particle movement feels. Obviously, $n_s(\vec{r}) = n(\vec{r})$. If V_s is

$$V_s = V + U + \left(T - T_s\right) \tag{13}$$

In this way, the assistant Kohn–Sham equation without interaction system can be solved.

$$\left[-\frac{\hbar^2}{2m}\nabla^2 + V_s(\vec{r})\right]\phi_i(\vec{r}) = \epsilon_i\phi(\vec{r}) \tag{14}$$

A series of electron orbital ϕ_i can be obtained. According to this, $n(\vec{r})$ the electron density of original multi-body can be solved.

$$n(\vec{r}) \equiv n_s(\vec{r}) = \sum_i^N \left|\phi_i(\vec{r})\right|^2 \tag{15}$$

Equivalent single-particle potential V_s can be expressed as

$$V_s = V + \int \frac{e^2 n_s(\vec{r})}{|\vec{r} - \vec{r}'|} d^3r' + V_{XC}[n_s(\vec{r})] \tag{16}$$

Where the second item is Hartree item describing Coulomb repulsion among electrons and the last item V_{XC} is called exchange-correlation potential including interaction of all multi-particles. Since both Hartree item and the exchange-correlation item V_{XC} depend on $n(\vec{r})$ and ϕ_i, and ϕ_i relies on V_s. Solutions to Kohn–Sham equation need use self-consistency method. Usually, an initial $n(\vec{r})$ is assumed first. Then, calculate corresponding V_s and solve ϕ_i in Kohn–Sham equation. Next, new density distribution can be calculated and start a new calculation. This process is repeated constantly until computed results are convergent.

In DFT, all approximations are integrated at the item that is called exchange-correlation energy. Thus, accuracy of DFT is decided by approximate forms of exchange-correlation energy functional directly. Thus, looking for better exchange-correlation approximation becomes a mainline for development of DFT system. An original simple approximation of exchange-correlation energy functional is local-density approximation (LDA), i.e., exchange-correlation functional of uniform electron gas with the same density is used as corresponding approximate value of non-uniform system. Unexpectedly, such a simple approximation usually brings good results, which directly leads to the situation that DFT is

widely applied later. Improvement based on LDA involves generalized gradient approximation (GGA). Under GGA, exchange-correlation energy is function of electron density and its gradient. A famous GGA functional constructed on the basis of this concept is PBE functional, which is one of the GGA fonctionelles that have been used most widely now. DFT calculation based on LDA or GGA constitutes the most popular calculation scheme of electron structure at present.

Besides, DFT has new development in many aspects. For instance, conventional DFT usually have inaccurate estimation on energy gap of materials. Using GW approximation, we may obtain more accurate energy band structure and thus more accurate energy gap. In order to apply DFT to strongly correlated system, people expand it. The simplest expansion is LDA+U that is widely applied now. Current density functional theory (CDFT) is a method used to deal with interaction electron system under any strength magnetic field. Density functional perturbation theory and Berry phase theory can obtain many physical properties of system by carrying out the First-principles calculation for lattice dynamics and combining with phonon dispersion. DFT is an advanced method in calculation of electron structure in many fields and has been widely applied to calculation of solid state physics and become an effective way to solve material design and processing puzzles. According to this theory, people may explain experimental data and predict basic properties of crystals, such as new structure, binding energy and surface activity.

Chapter 3

Hydrate Structure Prediction in Carbon Dioxide-Water System

3.1 Introduction

Carbon dioxide is a common compound in the air, which is formed by two oxygen atoms and one carbon atom, connected by covalent bonds. It's slightly soluble in water and can form carbonic acid. CO_2 can absorb infrared radiation, so it is a kind of greenhouse gas. As a large amount of greenhouse gas CO_2 are artificially discharged into the atmosphere, the climate gradually has become warmer over the past century. In nearly half a century, the sharp expansion of fossil fuel consumed by humans has resulted in constant rising of CO_2 concentration in the air. Before the industrial revolution, the CO_2 concentration was $280*10^{-6}$, but it has reached $387*10^{-6}$ now, and it is predicted to break through $500*10^{-6}$ by 2030. Because of the sluggishness (or inertness) of the climate system, plus there are more than $5\ 000*10^{15}$ gC fossil fuel resources, which will continue to be used by humans for a long time in the future, hence, the greenhouse effect caused by CO_2 emission obviously will last for centuries.[48] The greenhouse effect will have an adverse effect on global social economy in the future (such as water resource, agriculture, etc.), enable terrestrial and marine ecosystems to be destroyed (forest decline, frequent increase of drought and flood disasters, and some costal areas and islands submerged by rising sea level), and even menace human health.

Therefore, as a kind of gas hydrate, carbon dioxide hydrate has important value in research and application. Reducing CO_2 greenhouse gas in the air is an important way to effectively lessen global warming. Except for reducing the emission of CO_2 gas, recycling CO_2 in the air also is an important method to solve the problem. Seeking effective CO_2 recycling and storage methods is a goal strongly pursued by scientists in recent years, and it is a very feasible way to enclose CO_2 into clathrate water molecules to form gas hydrate and sink them to the bottom of the sea to seal up for safekeeping, on which many studies have been done. For instance, P.G. Brewer and others directly conducted CO_2 hydrate formation experiments in the sea, which indicated this method was operable.[49] T.Ebinuma and K.Ohgaki put forward the idea of displacing the methane in natural gas hydrate with CO_2, and E.M.Yezdimer and others calculated the change of free energy showing the possibility of this

method.[50,51] In addition, the formation process of CO_2 clathrate hydrate can be used to effectively separate CO_2 from other gases, which shows that researches on CO_2 gas hydrate are significant for environmental protection, energy and gas separation projects, etc. Hence, the study of carbon dioxide hydrate has always been a very active topic.

It is found in recent years that carbon dioxide hydrate is of CS-I type under low pressure. Dyadin's team once measured the dissociation curve of carbon dioxide hydrate, which showed evidence a second hydrate form that may exist at pressures above 0.6 GPa.[52] However, this research has not been verified with spectroscopic method.

3.2 Approach statement and parameter setting

The diversity of initial population of crystal structures plays an important role in the evolutionary algorithm. In that part of 天河 research, the parameters are set as following.

The number individuals in the initial population is 50; individuals of each generation is 50, the optimum 70% of the individuals are selected by functions to produce the next generation. Among the offspring structures, 40% of them are generated by heredity operators, 10% by rotation, and 40% by random selection. The fingerprint function is applied to obtain the symmetry property and remove the repetitive structures.

3.3 Structure of carbon dioxide hydrates

Based on the evolutionary algorithm USPEX, predicted crystal structure is were examined at of 5 GPa (0 K) in the carbon dioxide-water system, by variable composition calculation. The scheme of formation enthalpy and composition was determined to describe the relative stability of compounds formed by carbon dioxide and water with different stoichiometric ratio. The x-axis in the scheme represents composition ratio in carbon dioxide-water system, while the y-axis represents the average enthalpy per atom of different structures. The terminals at both sides are the reference phases for decomposition. In **Fig.6** (indexed as a convex hull diagram), the left end represents carbon dioxide, and the right end represents water. Both of carbon dioxide and water molecules are in solid form.

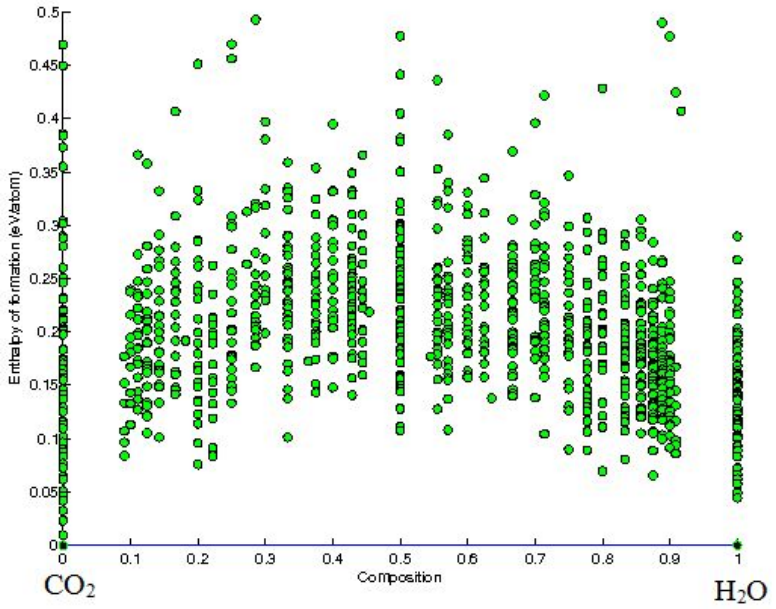

Fig. 6 Convex hull diagram of relative formation enthalpy for predicted crystal structures with variable composition in the carbon dioxide-water system. (5 GPa, 0 K)

The figure shows that, at pressure of 5 GPa, formation enthalpies of all the calculated structures formed by carbon dioxide and water is higher than the sum of the end member reference phases enthalpies. Therefore, the result indicates that there's no thermodynamically stable structure of carbon dioxide hydrate under the pressure of 5 GPa at 0 K.

Molecule	Enthalpy (eV/atom)
CO_2	-7.2143
H_2O	-4.7394

Table 1 The enthalpy (eV/atom) of CO_2 and H_2O (5 GPa, 0 K).

Table 1 lists the formation enthalpies (per atom) of carbon dioxide (solid) and water (ice), and **Table 2** lists the structures of which enthalpies are relatively lower among all the hydrates examined in the system. The formation enthalpy of $CO_2 \cdot 7H_2O$ is -120.6456 eV, while the the sum of enthalpy for one carbon dioxide and seven water molecules is -121.1703 eV. From the perspective of energetics, $CO_2 \cdot 7H_2O$ cannot stably exist under that condition. The other structure listed in **Table 2**, $CO_2 \cdot 4H_2O$, has a formation enthalpy of -78.1695 eV,

which is higher than that of one carbon dioxide and four water molecules (-78.5157 eV). Therefore, the structure is also thermodynamically unstable.

Structure	Enthalpy (eV/atom)	Enthalpy (eV)
$CO_2 \cdot 7H_2O$	-5.0269	-120.6456
$CO2 + 7H_2O$	-5.0488	-121.1703
$CO_2 \cdot 4H_2O$	-5.2113	-78.1695
$CO2 + 4H_2O$	-5.2344	-78.5157

Table 2 Comparison of formation enthalpy between carbon hydrates and reference phases. (5 GPa, 0 K).

The structures of the carbon dioxide hydrates are visualized by software, shown in **Fig.7** and **Fig.8**.

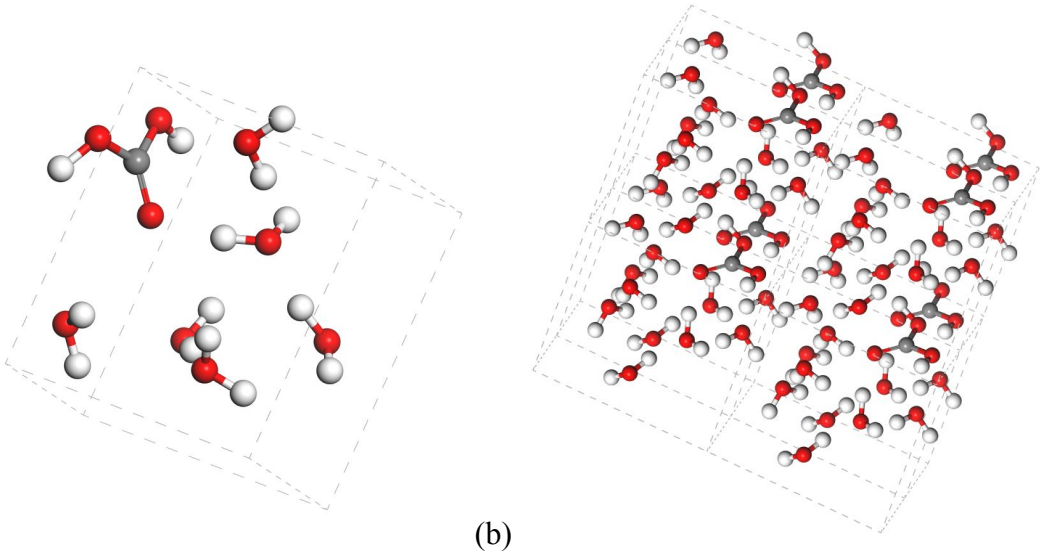

(a) (b)

Fig. 7 (a) Unit cell of $CO_2 \cdot 7H_2O$. gray balls represent carbon atoms, red balls represent oxygen atoms, and white balls represent hydrogen (b) $CO_2 \cdot 7H_2O$ structure in 2*2*2 lattice range.

For $CO_2 \cdot 7H_2O$, the crystal is triclinic, with symmetry group of P1. The figure also indicates that the carbon dioxide molecule has reacted with water to form carbonic acid, H_2CO_3. Information about the lattice is shown in **Table 3**.

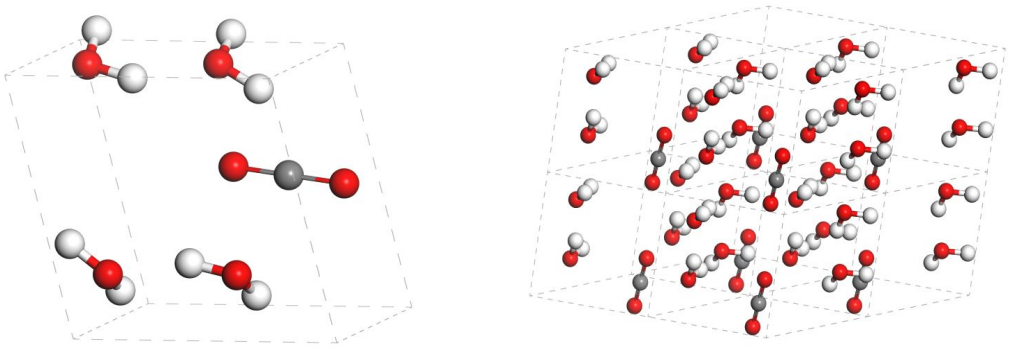

(a) (b)

Fig. 8 (a) Unit cell of $CO_2 \cdot 4H_2O$. gray balls represent carbon, red balls represent oxygen, and white balls represent hydrogen; (b) $CO_2 \cdot 4H_2O$ structure in 2*2*2 lattice range.

For the $CO_2 \cdot 4H_2O$ structure, the crystal is triclinic, and the symmetry group is P1. Lattice information is also listed in **Table 3.**

Structure	Lattice Parameter		Atom Position
$CO_2 \cdot 7H_2O$	a=4.328 Å	α = 95.336°	Primitive-centered (0,0,0)
	b=7.369 Å	β = 105.300°	
	c=5.987 Å	γ = 102.933°	
$CO_2 \cdot 4H_2O$	a=5.785 Å	α = 88.655°	Primitive-centered (0,0,0)
	b=5.537 Å	β = 112.395°	
	c=4.504 Å	γ = 69.961°	

Table 3 The lattice information of carbon dioxide hydrates (5 GPa, 0K).

The hydrate structures found in this study are not consistent with the reported carbon dioxide hydrate structure (CS-I) under low pressures. The volume and solubility of the carbon dioxide molecule may contribute to the instability of carbon dioxide hydrate in this system. The analysis implies the ionization of carbon dioxide, and one interpretation is that the local configuration carbonate is easily formed.

3.4 Band structure and Density of State (DOS)

The analysis of band structure can be used to judge the metallic character of systems. In the band structure diagram, the intersection of the Fermi level and conduction band signifies the metallicity of the material; conversely, the non-intersection of Fermi level and conduction band implies that the material is a semiconductor or insulator. For a semiconductor, the apex of the valence band locates at the Fermi level, and the band gap is narrow; while the band gap of an insulator at the Fermi level is comparatively broader.

The DOS (Density of States) is another important property for analyzing structures, which shows the bonding characteristics.

As stated previously, in the carbon-dioxide system (5 GPa, 0 K), there's no thermodynamically stable clathrate hydrate, and the structure closest to being stable is $CO_2 \cdot 7H_2O$. In this part, the band structure and DOS of $CO_2 \cdot 7H_2O$ has been calculated and analyzed by CASTEP program.

As shown in **Fig.9**, the conduction band has not intersected with Fermi level. The broad band gap shown in the DOS further verifies that $CO_2 \cdot 7H_2O$ is an insulator.

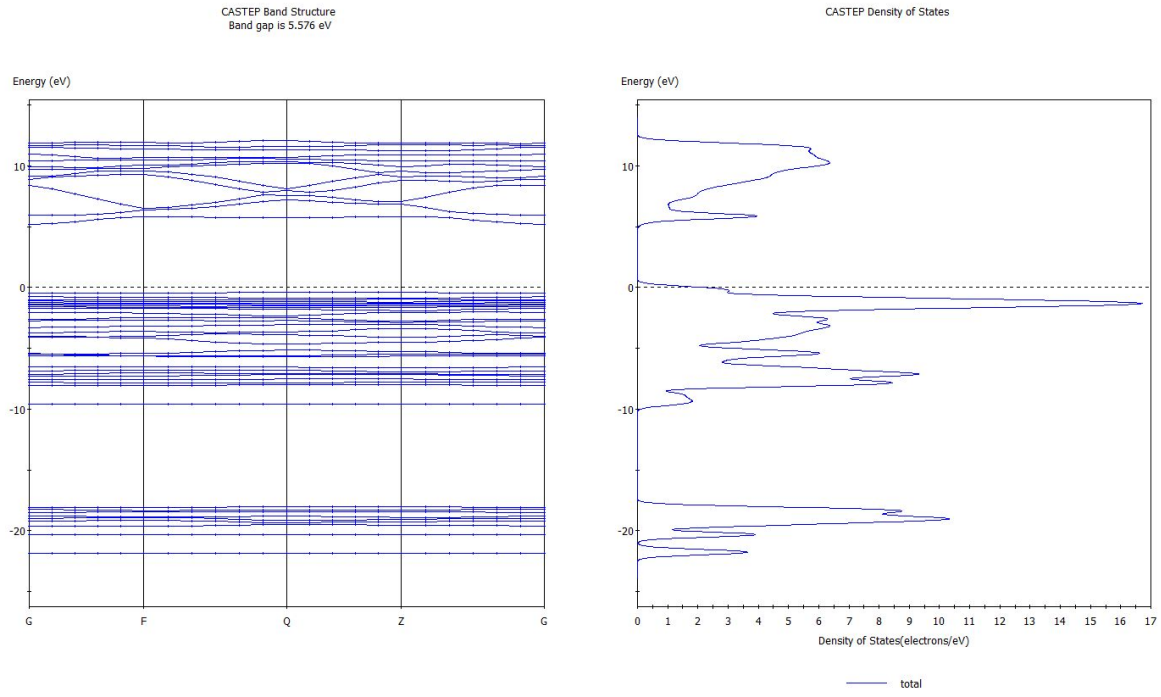

Fig. 9 Band structure and DOS of $CO_2 \cdot 7H_2O$ at 5 GPa (0 K)

Chapter 4

Hydrate Structure Prediction in Xenon-Water System

4.1 Introduction

Xenon is the only species of nonradioactive noble gases that is known to form a stable hydrate at ambient temperature. Even though it's a noble gas, its electronic shell may be polarized by the surrounding molecules, and produces biochemical effect with other biomolecules. As xenon has steady chemical properties, is nonirritant to the respiratory tract, and seldom metabolized through hepatorenal function, it has been often used as an anesthetic for complex cardiovascular surgeries.[53] However, its high price and high concentrations required restrict relevant studies. In recent years, the application of xenon at low temperature and high pressure has become a hot topic for research. If the steady configuration of xenon hydrate in different conditions can be further explored, the progress of application of xenon for clinical research will be promoted.

In the meantime, xenon hydrate may be used to explain the "missing Xe problem" in earth science. The ratio of Xe content in the atmosphere of the earth and Mars to other rare gases (such as neon, argon, krypton, etc.) is much less than expected, for which a possible explanation is that xenon forms compounds with rock and mineral compositions under some pressure.[54]

Currently, there have been some studies on the structure of xenon hydrates under different conditions. At low pressure, xenon hydrate adopts the CS-I structure type. In the DTA research, Dyadin and his group held that no stable xenon hydrates existed under above 1.5 GPa. However, using energy-dispersive methods, Sanloup and others found that xenon at pressures will change from CS-I into a new phase state near 1.8 GPa, with tetragonal structure hydrate and the ratio of water to xenon is 5.75:1; the hydrate decomposes when the pressure is increased to 2.9 GPa.[55] It was found in later studies that Xe-II actually was of SH type, and the proportion of xenon was higher than xenon hydrate of CS-I.[56] Research of Alavi and others found that larger cages in that structure contained two xenon atoms, and the ratio of water to xenon was 4.86:1.Further investigation found that xenon hydrate decomposes into ice and xenon at 2.9 GPa.[57]

4.2 Approach statement and parameter setting

The parameters settings for variable composition calculation are consistent under different pressures. The individuals of initial population is 50; 50 individuals in each generation, the optimum 70% of the individuals are selected to produce the next generation. 40% of the next generation is generated by heredity, 40% by random selection, 10% by rotation, and 10% by soft mutation.

For a fixed composition calculation of $2Xe \cdot 8H_2O$, the parameters are as following: 30 individuals in the initial population; 30 individuals in every generation, the optimum 70% of the individuals are selected for producing off-spring. 40% of the offspring population is produced by heredity , 30% by random selection, 20% by rotation, 10% by soft mutation.

4.3 Structure of xenon hydrates

Crystal structure prediction in the xenon-water system is performed at pressures of 10GPa, 20GPa and 50GPa (0 K). The convex hull diagrams are shown in **Fig.10** and **Fig. 13**. In these diagrams, the terminal at left side represents xenon (solid phase), while the terminal at right side represents water (ice).

Molecule	Enthalpy(eV/atom) -10GPa	Enthalpy(eV/atom) -20GPa	Enthalpy(eV/atom) -50GPa
Xe	2.7881	5.5709	10.6347
H_2O	-4.5349	-4.1326	-3.3682

Table 4 The enthalpy (eV/atom) of xenon and H_2O under different pressures and 0 K.

4.3.1 Structure of xenon hydrate at 10 GPa

Variable Composition Calculation

At a pressure of 10 GPa (0 K), the convex hull diagram and the formation enthalpy, which is calculated by USPEX and shown in **Table 5**, indicates that no stable structure of xenon

hydrate exists in that system at these conditions; but $2Xe \cdot 8H_2O$ can be regarded as a metastable structure.

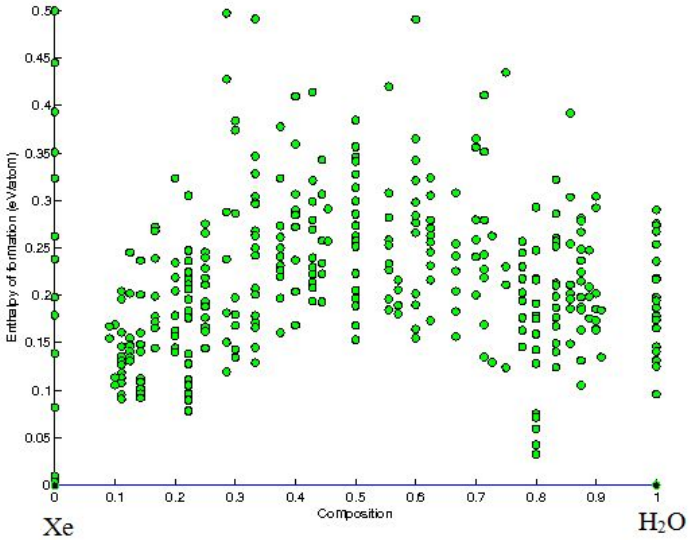

Fig. 10 Convex hull diagram of relative formation enthalpy for predicted crystal structures with variable composition in the xenon-water system. (10 GPa, 0 K)

Structure	Enthalpy (eV/atom)	Enthalpy (eV)
$2Xe \cdot 8H_2O$	-3.9591	-102.9366
$2Xe + 8H_2O$	-3.9717	-103.2641

Table 5 Comparison of formation enthalpy between xenon hydrates and reference phases. (10 GPa,0 K)

Fixed Composition Calculation

To examine the stability of $2Xe \cdot 8H_2O$, fixed composition calculations are performed at pressures of 10 GPa and 5 GPa (0 K). The best structures with lowest formation enthalpies of $2Xe \cdot 8H_2O$ are obtained from results, and their enthalpies are -102.935 eV (at 10 GPa) and -109.921 eV (at 5 GPa). By computing and comparison, the enthalpies are verified to be higher than that of the stable end member phases, which means that $2Xe \cdot 8H_2O$ remains a metastable state at either 10 GPa or 5 GPa.

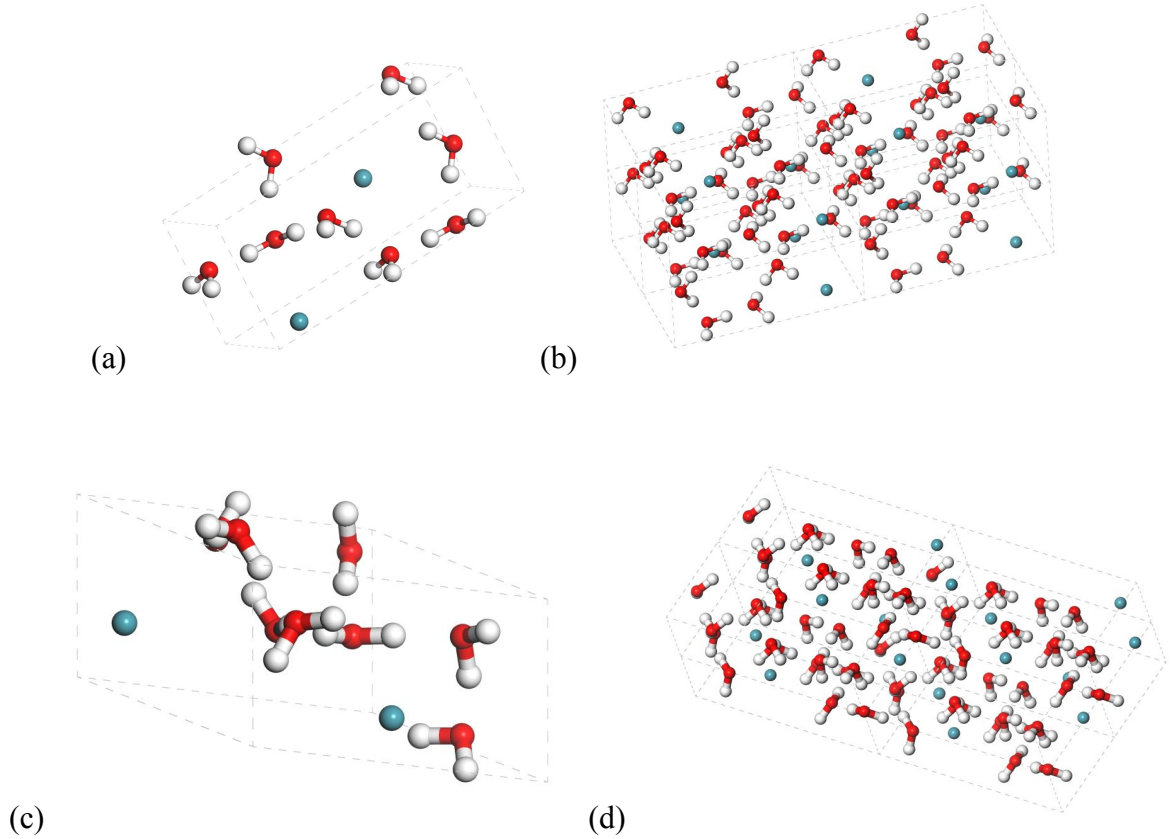

Fig. 11 (a) Unit cell of $2Xe \cdot 8H_2O$ at 10 GPa. blue balls represent xenon atoms, red balls represent oxygen atoms, and white balls represent hydrogen; (b) $2Xe \cdot 8H_2O$ structure in 2*2*2 lattice range at 10 GPa; (c) Unit cell of $2Xe \cdot 8H_2O$ at 5 GPa; (d) $2Xe \cdot 8H_2O$ structure in 2*2*2 lattice range at 5 GPa;

The structures of $2Xe \cdot 8H_2O$ under 10 GPa and 5 GPa are shown in **Fig.11**. Both are triclinic, with symmetry group of P1. The lattice parameters are shown in **Table 6**.

Structure	Lattice Parameter		Atom Position
$2Xe \cdot 8H_2O$ (10 GPa)	a=10.061 Å	α = 90.198°	Primitive-centered (0,0,0)
	b=4.633 Å	β = 90.892°	
	c=4.457 Å	γ = 88.872°	
$2Xe \cdot 8H_2O$ (5 GPa)	a=10.173 Å	α = 110.351°	Primitive-centered (0,0,0)
	b=4.317 Å	β = 89.954°	
	c=5.977 Å	γ = 90.107°	

Table 6 The lattice information of xenon hydrates at 10 GPa and 5 GPa. (0 K)

Band structure and Density of States (DOS)

The band structure and DOS was calculated by CASTEP program for further investigation of the properties of $2Xe{\cdot}8H_2O$. As shown in **Fig.12**, the $2Xe{\cdot}8H_2O$ under both sets of conditions adopts a broad band gap at Fermi level. Thus, it can be concluded that $2Xe{\cdot}8H_2O$ is an insulator. Moreover, the structure of conduction band, valence band and the electron density in **Fig.12(a)** and **Fig.12(b)** has shown consistency. Therefore, we can infer that the bonding characteristics of $2Xe{\cdot}8H_2O$ are similar at 5 GPa and 10 GPa.

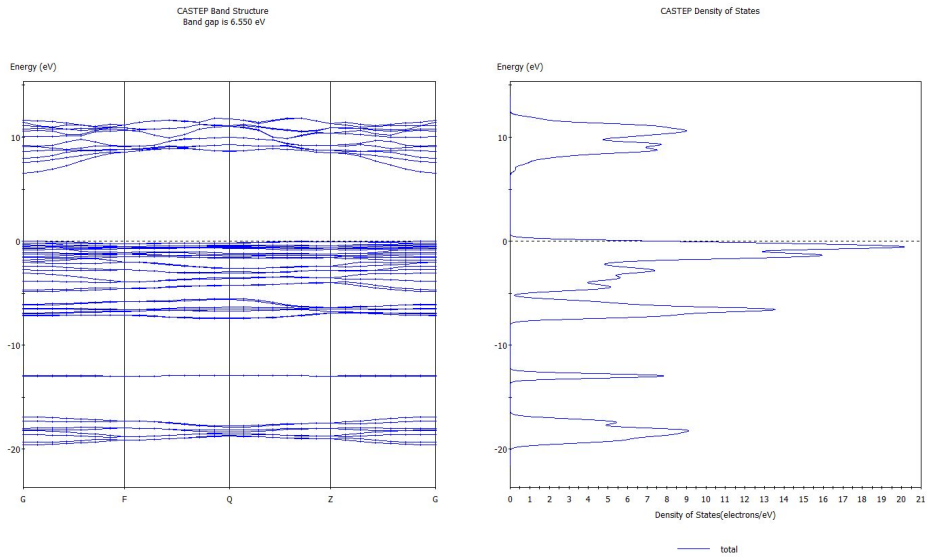

(a)

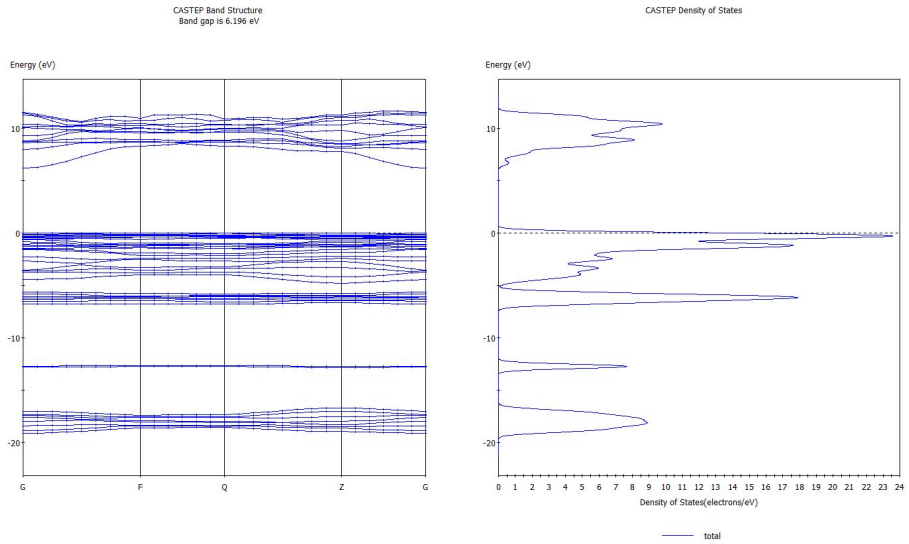

(b)

Fig. 12 (a) Band structure and DOS of $2Xe{\cdot}8H_2O$ at 10 GPa (0 K); (b) Band structure and DOS of $2Xe{\cdot}8H_2O$ at 5 GPa (0 K).

4.3.2 Structure of xenon hydrate at 20 GPa and 50 GPa

The results of variable composition calculations conducted under 20 GPa and 50 GPa (**Fig. 13**) illustrate that xenon cannot form stable nor metastable structures under such circumstances.

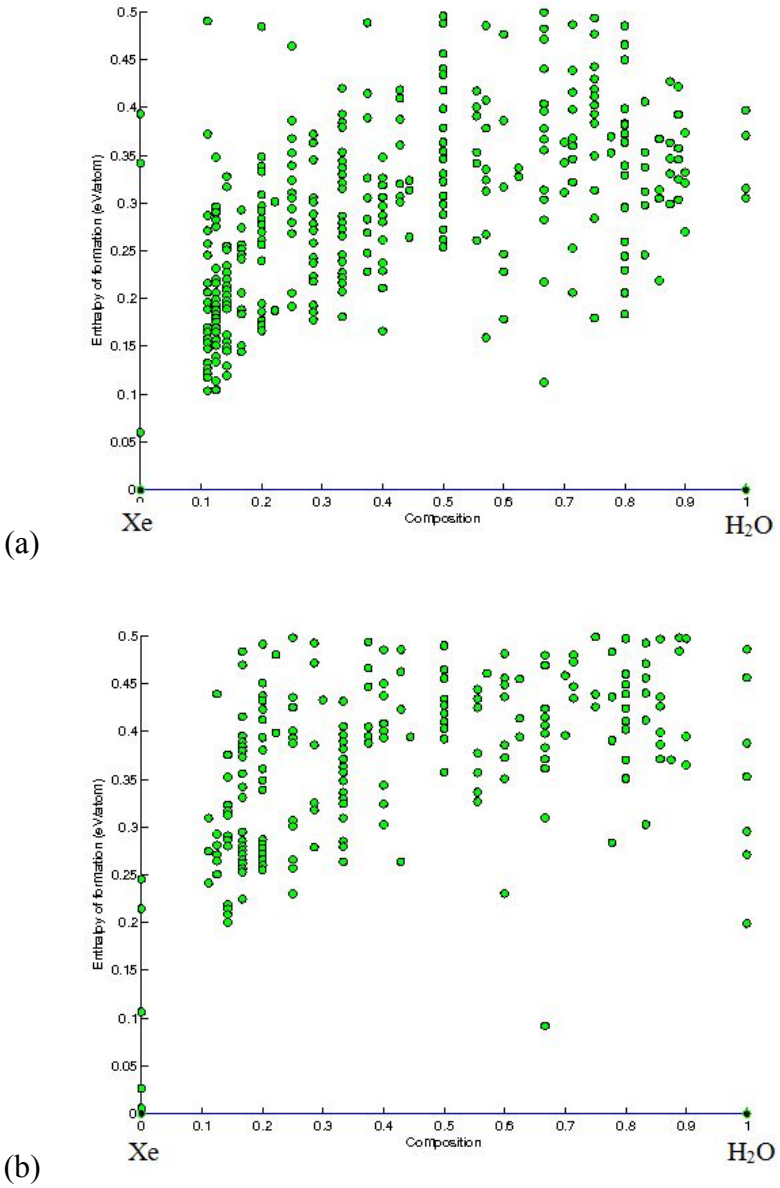

Fig. 13 (a)Variable composition for enthalpy in the xenon-water system at 20 GPa (0 K); (b)Variable composition for enthalpy in the xenon-water system at 50 GPa (0 K).

The best structures sharing the lowest formation enthalpy are listed in **Table 7**. The formation enthalpy of $2Xe{\cdot}4H_2O$ is much higher than that of the stable end member phases. The hydrate may decompose easily to water and xenon.

Structure		Enthalpy (eV/atom)	Enthalpy (eV)
20 GPa	$2Xe{\cdot}4H_2O$	-2.6983	-37.7762
	$2Xe + 4H_2O$	-2.7464	-38.4494
50 GPa	$2Xe{\cdot}4H_2O$	-1.3284	-18.5976
	$2Xe + 4H_2O$	-1.3678	-19.149

Table 7 Comparison of formation enthalpy between xenon hydrates and reference phases at 20 GPa and 50 GPa. (0 K)

4.3.3 Conclusion of xenon hydrate

The metastable structure $2Xe{\cdot}8H_2O$ found at pressures of 5 GPa and 10 GPa is different from the xenon hydrate structures (CS-I and SH) reported in the literature. And nor is it consistent with the other types of known clathrate hydrate structures (CS-II and ST), which could be taken as further evidence for its instability. With increasing pressure, the hydrates in the xenon-water system indicate a tendency of instability.

References

[1] S. Fan, T. Guo, *Chemical Industry and Engineering Progress,*1999, 1, 5-7.

[2] H. Davy, *Philos.Trans.R.Soc.London*, 1811, **101**, 1-35.

[3] E. G. Hammerschmidt, *Ind.Eng.Chem.*, 1934, **268**, 851-855.

[4] E. D. Sloan, *Clathrate hydrates of natural gases*, Marcel Dekker, New York, 2nd edn, 1998.

[5] V. R. Belosludov, M. Y. Lavrentiev, Y. A. Dyadin and S. A. Syskin, *Izv.Akad.Nauk SSSR*, Ser.Khim., 1989, **6**, 49-56.

[6] M. Von Stackelberg and H. R. Muller, *J.Chem.Phys*., 1951, **19**, 1319-1320.

[7] H. R. Muller and M. Von Stackelberg, *Naturwissenschaften*, 1952,**39**, 20-21.

[8] M. Von Stackelberg and H. R. Muller, *Naturwissenschaften*, 1951,**38**, 456-456.

[9] K. A. Udachin, C. I. Ratcliffe, G. D. Enright and J.A.Ripmeester, *Supramol.Chem.*, 1997, **8**, 173-176.

[10] H. S. Kim and G. A. Jeffrey, J.Chem.Phys., 1970, 53, 3610-3615.

[11] J .S. Loveday and R. J. Nelmes, *Phys.Chem.Chem.Phys.*, 2008, **10**, 937-938

[12] Y. A. Dyadin, E. Y. Aladko and E. G. Larionov, *Mendeleev Commun.*, 1997, **7**, 34-35.

[13] J .S. Loveday and R. J. Nelmes, *Phys.Chem.Chem.Phys.*, 2008, **10**, 938-948

[14] Y. A. Dyadin, E. G. Larionov, T. V. Mikina and L. I. Starostina, *Mendeleev Commun.*, 1997, **7**, 74-76.

[15] Y. A. Dyadin, E. G. Larionov, D. S. Mirinski, T. V. Mikina and L.I. Starostina, *Mendeleev Commun.*, 1997, **7**, 32-34.

[16] Y. A. Dyadin, E. G. Larionov, A. Y. Manakov, F. V. Zhurko, E. Y. Aladko, T. V. Mikina and V. Y. Komarov, *Mendeleev Commun.*, 1999, **9**, 209-210.

[17] Y. A. Dyadin, E. Y. Aladko, A. Y. Manakov, F. V. Zhurko, T. V. Mikina, V. Y. Komarov and E. V. Grachev, *J.Struct.Chem.*, 1999, **40**, 790-795.

[18] Y. A. Dyadin, E. G. Larionov, E. Y. Aladko and F. V. Zhurko, *Dokl.Phys.Chem.*, 2001, **378**, 159-161.

[19] H. Hirai, T. Kondo, M. Hasegawa, T. Yagi, Y. Yamamoto, T. Komai, K. Nagashima, M. Sakashita, H. Fujihisa and K. Aoki, *J.Phys.Chem.B*, 2000, **104**, 1429-1433.

[20] Martoncaron, *et al*., *Physical Review Letters,* 2003. **90**, 075503.

[21] J. Maddox, *Nature*, 1988, **335**(6187), 201-201.

[22] F. J. DiSalvo, *Science*, 1990, **247**(4943), 649-655.

[23] F. C. Hawthorne, *Nature*, 1990, **345**(6273), 297-297.

[24] J. Pannetier, *et al*., *Nature,* 1990. **346**(6282), 343-345.

[25] C. R. A. Catlow and G. D. Price, *Nature*, 1990. **347**(20), 243-248.

[26] M. U. Schmidt and U. Englert, *Chem.Soc.*, 1996. **10**, 2077-2082.

[27] M. A. C. Wevers, *et al.*, Solid State Chem. 1998. **136**, 233-246.

[28] M. Jansen, *Chem.Int.Ed.*, 2002. **41**, 3746-3766.

[29] J. C. Schön and M. Jansen, *Z. Kristallogr.*, 2001. **216**, 307-325.

[30] J. C. Schön and M. Jansen, *Z. Kristallogr.*, 2001. **216**, 361-383.

[31] M. W. Lufaso and P. M. Woodward, *Acta Cryst.B.*, 2001, **57**, 725-738.

[32] A. L. Bail, J.Appl.Crystallogr, 2005, 38, 389-395.

[33] C. M. Draznieks, *et al., Angew.Chem.Int.Ed.,* 2000, **39**,2 270-2275.

[34] C. M.Drazniek, et al., *Chem.Eur.J*. 2002, **8**, 4102-4113.

[35] Q. Zhu, *et al.*, *Phys. Rev. B.* 2011. **83**, 193410.

[36] X. D. Wen, et al., *Proc. Natl Acad. Sci.* 2011, **108**, 6833-6837.

[37] V. L. Solozhenko, *et al.* , *Journal of Superhard Materials*, 2008, **30**, 428-429.

[38] A. R. Oganov, *et al.*, Nature, 2009. 457, 863-867.

[39] A. R. Oganov., *Modern methods of crystal prediction,* Wiley-VCR, 2010.

[40] A. O. Lyakhov, A. R. Oganov, H.T. Stokes, Q. Zhu, *Computer Physics Communications,* 2013, **184**, 1172-1182.

[41] A. R.Oganov, Y. Ma, C. W. Glass, M. Valle, *Psi-k Newsletter*, 2007,144-145.

[42] M. D. Segall， P. J. D. Lindan, M. J. Prober, *et a1*., *J. Phys.Coudens.Matt.*， 2002, 14, 2717—2743.

[43] J. Chen, X. Chen, W. Zhang and J. Zhu, *Chinese Physics B*, 2008, **17**,1377-1379

[44] P. Hohenberg and W. Kohn, *Phys. Rev*., 1964, **B136**, 864-871.

[45] J. C. Slate, *Self-Consistent field for molecular and solids: quantum theory of molecular and solids*, McGraw-Hill, New York, 1974, 20.

[46] W. Kohn and L.J. Sham, *Phys. Rev.*, 1965, **A140**, 1131-1138

[47] J. A. Pople, P. M. W. Gill, and B. G. Johnson, *Chem. Phys. Lett*., 1992, **199**, 557-560.

[48] Q. Shi, W. Guo, Y. Han and M. Hu, *Marine Science Bulletin*, 2005, **24**, 72-73.

[49] P. G. Brewer, G. Fiederich，E. T. Peltzer, *et a1*., *Science,* 1999, **284**, 943-945.

[50] T. Ebinuma, *Method for dumping and disposing of carbon dioxide gas and apparatus therefore*, us:5261490, 1993.

[51] K. Ohgaki, H. Sangawa, T. Matsubara, *et a1*., *J. Chem. Eng. Japan.*, 1996，**29**, 478-481.

[52] Y. A. Dyadin, E. G. Larionov and A. Y. Manakov, *Gas hydrates at high pressures—State of the art*, in Proceedings of the Fourth International Conference on Gas Hydrates, ICGH Yokohama, Yokohama, 2002, pp. 590-594.

[53] E. Eger, B. Brandstater, L. J. Saidman, et al., *Anesthesiology*, 1965, **26**, 771-777.

[54] E. Anders and T. Owen, *Science*, 1977, **198**, 453-465.

[55] C. Sanloup, H. K. Mao and R. J. Hemley, *Proc. Natl. Acad. Sci. U. S. A.*, 2002, **99**, 25-28.

[56] W. L. Vos, L. W. Finger, R. J. Hemley and H. K. Mao, *Chem. Phys. Lett.*, 1996, **257,** 524-530

[57] S. Alavi, J. A. Ripmeester and D. D. Klug, *J. Chem. Phys.*, 2006, **125**, 104501.